DENTAL MATERIALS 38 (2022) 670–679

Available online at www.sciencedirect.com

ScienceDirect

journal homepage: www.elsevier.com/locate/dental

Tooth whitening effects on dental enamel, oxidation or reduction? Comparison of physicochemical alterations in bovine enamel using Synchrotron-based Micro-FTIR

Clara Babot-Marquillas[a,1], *Maria-Jesús Sánchez-Martín*[a,*,1], *Jose Manuel Amigo*[b], *Ibraheem Yousef*[c], *Iris H.Valido*[a], *Roberto Boada*[a], *Manuel Valiente*[a]

[a] *IKERBASQUE, Basque Foundation for Science, 48011 Bilbao, Spain*
[b] *Department of Analytical Chemistry, University of the Basque Country, P.O. Box 644, 48080 Bilbao, Basque Country, Spain*
[c] *ALBA Synchrotron Light Source, 08193 Cerdanyola del Vallès, Spain*

ARTICLE INFO

Article history:
Received 15 February 2021
Received in revised form 10 January 2022
Accepted 15 February 2022

Keywords:
Tooth whitening
Sodium metabisulphite
Liposomes
Synchrotron
MicroFTIR
PCA

ABSTRACT

Objectives: To compare the side effects of typical whitening treatments (by means of oxidation) compared to the new treatment developed by the authors through reduction. The aim is to provide information about the chemical interactions of the encapsulated reductant agent (metabisulfite, MBS) with the enamel structure compared with carbamide peroxide (CP) and to study their penetration in the hydroxyapatite (HAP) and the changes produced in the mineral and its hardness.

Methods: Chemical imaging is performed by synchrotron-based micro Fourier transformed infrared spectroscopy (SR-μFTIR). Continuous Stiffness Measurements (CSM) were used to determine the depth reached by the treatments in order to delimitate the area of study.

Results: The SR-μFTIR studies showed that MBS treatments softened the first 10 μm of enamel, as happens in the initial stages of tooth decay. Principal component analysis (PCA) showed that the main differences between treatments were found in the intensity of the ν_3 PO_4^{3-} peak related to tooth demineralization. CP and MBS promoted different changes in the HAP mineral, observed as opposite shifts of the peak: CP shortened the P-O bond while MBS seemed to elongate it. Moreover, MBS promoted the loss of carbonates while CP did not, which is probably related to the solution's pH. When comparing MBS and MBS Liposomes, it was observed how liposomes favoured the diffusion of MBS to inner layers, since the effects of MBS were observed in deeper enamel. Thus, the encapsulated MBS whitening effect is highly improved in terms of time when compared to MBS alone or CP.

* Corresponding author.
E-mail address: mariajesus.sanchez@uab.cat (M.-J. Sánchez-Martín).
[1] Shared co-first authorship

https://doi.org/10.1016/j.dental.2022.02.006

Significance: The obtained results indicated that using oxidizing (CP) or reducing (MBS) treatments, promote different HAP mineral changes, and that liposomes favour the diffusion of MBS into the enamel. It is the first time that synchrotron light is used to map the bovine incisor's enamel chemically, and to determine the effect of a whitening treatment in terms of chemical HAP modifications, and the extent in deep of these effects.

1. Introduction

Tooth whitening (aka tooth bleaching) [1], is a widely practiced aesthetic treatment around the world. Its effects in terms of the whitening results are widely studied using colourimetric techniques [2], since the main goal is to change the colour, to obtain a bright, clean and white smile. However, besides the desired final aesthetic result, the bleaching treatment also has undesirable effects due to its mechanism of action. The whitening effect is based on the oxidizing power of peroxides, e.g. hydrogen peroxide (HP), or carbamide peroxide (CP), the latter is composed by urea and hydrogen peroxide molecules. HP decomposes in reactive oxygen species (ROS) that are highly oxidative [3]. It performs its action penetrating through the different tooth structures of the discoloured tooth reaching the adsorbed stains in the enamel and dentin, and the ROS break the double bonds of the staining molecules making them unable to absorb light [4]. Enamel and dentin behave as semi-permeable membranes allowing the diffusion of HP according to Fick's second law [5] reaching the pulp in minutes [6]. For CP, the urea groups degrade the organic parts of the enamel, leaving empty spaces that favour the diffusion of hydrogen peroxide throughout the whole enamel thickness [7]. Higher concentrations and longer application times are associated with better results [8], but also with a higher incidence of side effects like hypersensitivity (the most common secondary effect of dental whitening) [9] and pulp damage [5], tooth demineralization (leading to changes in roughness and hardness) and gingival irritation [7]. Besides, the need to apply these products for hours, either at the dentist or at home, is not convenient for the user.

Efforts have been made to find a solution to reduce HP concentrations and exposure times. Novel strategies avoiding the use of peroxides are also being explored. For instance, whitening based on piezocatalysis using $BaTiO_3$ nanoparticles and vibration showed whitening results after 10 h application [10]; the use of natural compounds like proteolytic enzymes (bromelain, papain and ficin) also showed visible results after 4 applications of 15 min each [11]. These solutions may solve the secondary effects derived from the peroxides, but not the inconvenience of long application times.

In previous works, we reported how an outstanding whitening was achieved by using a reducing agent, sodium metabisulphite (MBS), as bleaching agent when compared with the traditional oxidizing ones[12]. In addition, we found that the whitening effect increases when MBS is encapsulated in liposomes obtaining significant whitening results in 3 min [13]. Indeed, the purpose of these nanostructures is twofold, they act as a carrier of the MBS and, on the other hand, they create a layer over the enamel surface that improves the diffusion of the reductant towards the tooth. It was also seen that the encapsulated MBS had physical effects over the enamel, increasing the surface roughness within safe limits; nevertheless, the enamel-treatment chemical interaction was still pending to study.

Although mammalian enamels are similar, bovine enamel has some differences compared with the human one. It contains a larger number of fibril-like interprisms, and the average diameter of enamel crystals is bigger. It also has different decussating patterns, since in bovine enamel hydroxyapatite (HAP)crystallites within a rod are not merely parallel but twisting as fibres in a thread of wool [14]. Nevertheless, in the field of tooth whitening, bovine incisors are widely used as an *in vitro* model, since they are considered a valid model by ISO 28399 to test products for external tooth whitening treatments [15], since human incisors are quite difficult to obtain. In the present work, bovine incisors have been used as *in vitro* model.

When analyzing the side effects of whitening treatments on enamel, most of the studies are focused on determining the changes in its mechanical properties, like surface hardness or roughness; however, these techniques are not able to provide information about the chemical changes taking place in neither the inorganic nor the organic structures. Fourier transformed infrared (FTIR) spectroscopy is a molecular vibrational technique that has been shown to be advantageous to investigate mineralized tissues like teeth, providing information on the chemical structure at the molecular scale. The addition of a microscope to FTIR microspectroscopy (μFTIR) has led to the possibility of combining biochemical with spatial information, i.e., chemical imaging, which has the potential to examine tissues at cellular resolution [16]. The use of synchrotron radiation light sources, synchrotron-based FTIR microspectroscopy (SR-μFTIR), provides a much better signal to noise ratio [17], and the possibility of using a smaller beam size without losing signal efficiency [16] than when using traditional sources. SR-μFTIR in specular reflectance mode can provide very precise chemical information in small areas, therefore it is a very suitable technique to study the changes induced by whitening treatments and to characterize the extent of its effects with precision. Actually, it has been previously used to study the ablation in enamel caused of pulsed CO_2 lasers, allowing to detect ablations of 9 μm [18].

Since whitening treatments are applied directly on the enamel surface, the most affected parts in terms of chemical

transformations are the surface itself and the enamel immediately below, since these parts are exposed to the highest concentration of the oxidant. According to this, a study revealed that *in vitro* application of 10% CP on enamel for two weeks caused demineralization of the enamel extending to a depth of 50 µm below the enamel surface [19].

Here we report a SR-µFTIR study on the chemical changes induced in HAP by either oxidizing (CP) or reducing (MBS) whitening treatments in bovine incisors enamel, down to 50 µm depth from the surface. Besides, the chemical distribution of inorganic and organic species in the enamel of bovine incisor were mapped and studied by using multivariate analysis (principal component analysis, PCA). To our knowledge and up to date, no study has been reported using SR-µFTIR to determine the effects of MBS as a whitening treatment in terms of chemical HAP modifications, and the extent in deep of these effects. Neither the bovine incisor enamel has been chemically mapped using synchrotron light. The aim of this work is to provide information about the chemical interactions of the encapsulated reductant agent (metabisulfite, MBS) with the enamel structure compared with carbamide peroxide (CP) and to study their penetration in the hydroxyapatite (HAP) and the changes produced in the mineral and its hardness. Thus, to compare the side effects provoked by typical whitening treatments (by means of oxidation) compared to the new treatment developed by the authors (by means of reduction).

2. Materials and methods

2.1. Reagents

Tannic acid was purchased from Sigma-Aldrich (Missouri, USA), sodium metabisulfite from Riedel-de Haën (Seelze, Germany), all in powder form. Carbamide peroxide was obtained from Acros Organics (New Jersey, USA), in 1 g stabilized tablets (35% w/w H_2O_2). Dipalmitoylphophatidylcholine (DPPC) was purchased from Avanti Polar Lipids (Alabama, USA). All chemicals were of analytical grade. Deionized water was purified through a purification system from Millipore (Milford, MA, USA).

2.2. Treatments preparation

Deionized water was used as control. Sodium metabisulphite solution was at a concentration of 0.47 M (MBS). Carbamide peroxide solution (CP) was prepared at 16% (w/v). DPPC liposomes solution (lipos DPPC) was obtained by lipid film hydration [20] at a concentration of 20 mM of DPPC encapsulating water. MBS liposomes (MBS lipos) solution was obtained by monolayer technique at 20 mM of DPPC encapsulating a solution of metabisulphite at 0.47 M. The pH of the different treatments is reported in Table 1.

Table 1 – Treatment's pH values at 25 °C.

Treatment	pH
H_2O	6.5
DPPC lipos	5.7
MBS	2.9
MBS lipos	2.4
CP	8.0

2.3. Sample preparation

2.3.1. Samples for continuous stiffness measurement

Ten specimens (2 specimens for treatment) of bovine incisors were cleaned of gross debris, and the root was sectioned using a diamond saw and preserved in sodium azide solution (0.2%) until the experiment performance. Teeth were embedded in self-curing polyacrylic cylinders. Their surface was polished to expose a window of at least 3 × 3 mm of the enamel surface, which permitted the Continuous Stiffness Measurements (CSM). The polishing was done using a sequence of silicon carbide paper starting at grit size P400 and sequentially increasing to P4000, under a constant flow of tap water, and afterwards with a sequence of diamond pastes with a mean particle size of 3 and 1 µm followed by a slurry of aluminium oxide with a mean particle size of 0.3 µm. After every polishing step, the samples were submerged in deionized water and sonicated for 30 s. The different whitening treatments were freshly prepared and applied for 20 min on the flattened surface of the specimens.

2.3.2. Samples for SR-µFTIR

Five bovine incisors (1 specimen per treatment) were used; each tooth was immersed in the corresponding freshly prepared treatment for 20 min making sure that only the enamel was in contact with the solution, avoiding the penetration of the treatment through the root cut part where the pulp is exposed, and then brushed for 30 s with an electric toothbrush (Oral-B Vitality Serie, BRAUN) while rinsed with distilled water. Afterwards, the specimens were embedded in an acrylic resin, and cut vertically along the central lobe to obtain a mesial view from the inside, the exposed surface was polished up to 1 µm particle size as described in Section 2.3.1, in order to obtain proper reflection properties for the measurements.

2.4. Continuous stiffness measurement

The dynamic continuous stiffness method (CSM) permits to investigate the dependence of the dynamic hardness as a function of the penetration depth during a nanoindentation. CSM was performed with a Nano Indenter® XP from MTS (Tenessee, USA) using a Berkovich diamond tip. Nine measurements per sample were performed separated 100 µm between them. Before every measurement, the diamond indenter was calibrated on a standard fused silica specimen.

2.5. Specular reflectance SR-µFTIR measurements

Specular reflectance spectra were acquired using the FTIR microscope in the reflection mode at MIRAS beamline of ALBA synchrotron light source (Cerdanyola del Vallès, Spain) [21], using a Hyperion 3000 microscope coupled to a Vertex 70 spectrometer (Bruker, Germany), and equipped with a Mercury-Cadmium-Telluride (MCT) detector. The microscope is

utilizing a 36x Schwarzschild objective (NA = 0.52) coupled to a 36x Schwarzschild condenser to focus the synchrotron IR light on the sample. OPUS 7.5 (Bruker, Germany) was used to collect the spectra, taking a minimum of 256 co-added scans per spectrum in the 650–4000 cm^{-1} Mid-IR range and with a 4 cm^{-1} spectral resolution, using a 5 × 5 μm^2 masking aperture size. A gold mirror reference was used as reference to collect the background.

To characterize bovine enamel physiological variations, a mapping of the whole enamel thickness, of 500 µm long and 50 µm width, was performed in the mid crown (labial side) of the control sample. To observe the effect of the enamel surface in treated samples, mappings of the outer enamel region, of 50 × 50 µm, were performed also in the mid crown (labial side), starting in the enamel surface and moving towards the dentin direction. Spectra measurements were taken in spots separated by 10 µm each, resulting in a matrix of 50 × 6 points in the control and 6 × 6 points in the treated samples.

2.6. Data treatment

Principal component analysis (PCA), a multivariate method, widely used in hyperspectral images [22] aims at extracting the major sources of variance (variability) in the map of the sample. This variance correlates, to some extent, with the chemical compounds conforming the sample, giving an indication of the compounds' distribution along the surface in an unsupervised and straightforward manner. In the present work, PCA was applied by using HYPER-Tools version 2 [23].

In the spectral data obtained for this study, the most intense peak is the ν_3 PO_4^{2-}. It has been already reported that when dentin is treated with acids, its intensity is insufficiently constant for normalization [24], causing artefacts in the normalized spectra. However, the spectra were mean centered before the PCA analysis in order to homegeize the variariance between the variables. A total of 625 spectra (an area of 25 ×25) were measured per sample. The Unscrambler X® (2016, CAMO Software AS, Norway) was used to assign peak spectra numbers and to perform maximum normalizations when needed to observe the peak shifts. The chemical mapping was performed by integrating the peak area with integration mode A (bordered by the spectrum curve, the x-axis and the two wavenumber limits (700–1700 cm^{-1}) defined, using the software OPUS 7.5 (Bruker, Germany).

3. Results

3.1. Peaks assignment

The bands corresponding to carbonates and phosphates of the HAP forming the enamel have been identified (Fig. 1) in a control sample.

The broad absorption bands in the 1170–965 cm^{-1} region correspond to the apatitic phosphate groups coming from a triply degenerated asymmetric stretching mode ($\nu_3PO_4^{3-}$) [25]. Its deconvolution is described in the literature as secondary phase vibrations of Ca-O-P at 1103 cm^{-1}, P-O at 1091 cm^{-1}, Ca-O at 1047 cm^{-1} and O-Ca-O at 1031 cm^{-1} [26] (typically occurring in stoichiometric apatite with a relation $Ca_{10}(PO_4)_6(OH)_2$ [27]). The band at 956 cm^{-1} corresponds to the symmetric stretching mode of phosphate ($\nu_1PO_4^{3-}$) [25]. The region between 1580 and 1320 cm^{-1} corresponds to $\nu_3CO_3^{2-}$ antisymmetric stretching; in this band two maxima can be observed, at 1401 and 1442 cm^{-1}, whose intensities are slightly different, being the peak at 1401 cm^{-1} a little higher; also a peak at 1540 cm^{-1} (region 1535–1565 cm^{-1}), corresponding to $\nu_3CO_3^{2-}$ and organic material (amide II), was detected [28]. Another carbonate band arises at 880–830 cm^{-1}, corresponding to the out-of-plane bending mode of the C–O bond ($\nu_2CO_3^{2-}$ group) [28–31]. When the carbonate substitutes the hydroxyl group it is designated as type A apatite and when it substitutes the phosphate group it is designated as type B apatite, and it is described that there are equal amounts of A and B in dental enamel [32]. According to Brangule *et.al.* [33] peaks' deconvolution, there is a peak doublet at 1540 and 1455 cm^{-1} corresponding to type A carbonates and a doublet at 1475 and 1416 cm^{-1} corresponding to type B; for the $\nu_2CO_3^{2-}$ band, a peak at 880 cm^{-1} is assigned to type A and other at 871 cm^{-1} to type B. This means that the peaks in the regions 1580–1320 cm^{-1} and 880–830 detected in the reflection mode are showing a mixture of type A and B carbonates, except for the peak at 1540 cm^{-1} that reflects type A as well as organic matter.

3.2. Chemical distribution in incisor bovine enamel

The characteristic distribution of crystals in dental enamel confers its distinctive mechanical properties, like its exceptional elasticity and resilience [34]. It must be remarked that enamel is not homogeneous but an anisotropic material, showing spatial variations in its chemical composition and density, as well as variations in the carbonate content and the degree of crystallinity [35].

To evaluate the chemical distribution of carbonates and phosphates, an area of non-treated bovine tooth enamel was fully mapped by SR-µFTIR from the surface to the dentino-enamel junction (DEJ) along a cross-section of 500 µm long and 60 µm wide (Fig. 2). For the sake of clarity, the intensity of the colour scale is adjusted to the intensity of the corresponding highest peak.

Phosphate (PO_4^{3-}) is the principal molecular species that gives rise to the HAP absorbance in the 900–1200 cm^{-1} region, and its distribution can be seen from the integration of ν_3 antisymmetric and ν_1 symmetric stretching vibrations. For ν_3 PO_4^{3-}, the peak intensity is higher (white area) in the mantel of the enamel. Moreover, it is progressively reduced as it goes deeper in the enamel (Fig. 2), and a dramatic reduction of the intensity is observed in the dentin since its phosphate content is lower and its crystallinity decreases [36].

For ν_1 PO_4^{3-}, high intensity spots were observed in several places along the enamel; Pleshko N. et al. found a direct relationship between the percentage area of the v_1 band (near 960 cm^{-1}) and the crystal size [37], therefore those regions could correspond to discrete areas with larger crystals. Carbonates showed complementary intensity distribution to the phosphates, with the highest intensity close to the dentin and lower in the outer part of the enamel. This is in accordance with previous works reporting that the carbonate

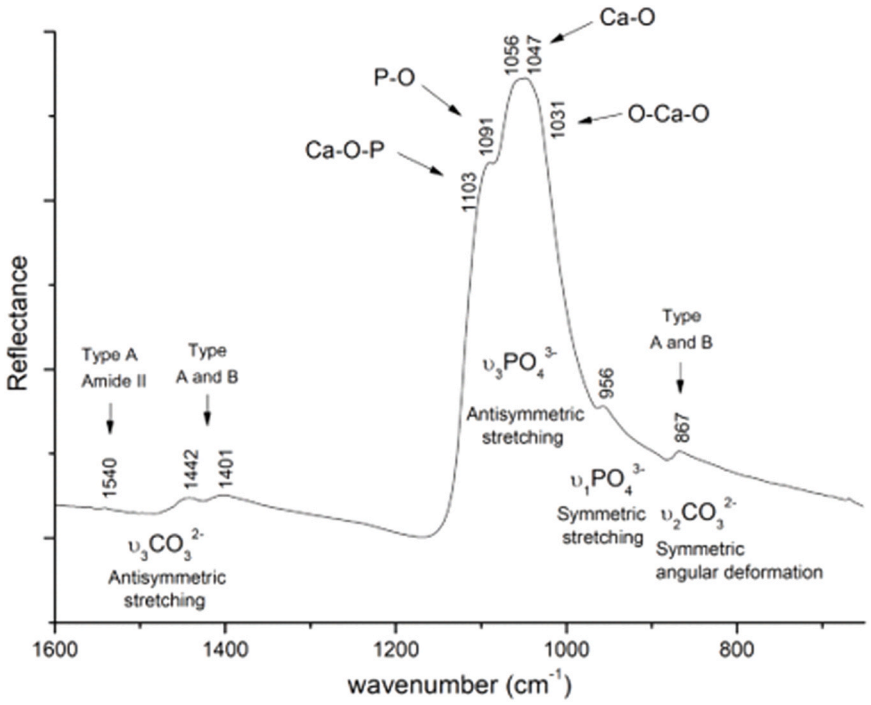

Fig. 1 – Specular reflectance FTIR (carbonated hydroxyapatite) spectrum of enamel and band assignment numbers (original figure). The spectrum corresponds to the average of 6 spectrum measured in the first 10 µm of control's outer enamel.

content increases from outer to inner enamel in bovine incisors [38]. Comparing the regions 1580–1320 cm^{-1} and 880–830 cm^{-1}, corresponding to the two types of vibration of the carbonate group (antisymmetric stretching and symmetric angular deformation), similar intensity patterns can be observed (note the similar intense point at around 400 µm

Vibration	$v_3\ PO_4^{3-}$	$v_1\ PO_4^{3-}$	$v_3\ CO_3^{2-}$		$v_2\ CO_3^{2-}$
Range (cm^{-1})	1160-965	965-935	1530-1550	1580-1320	880-830

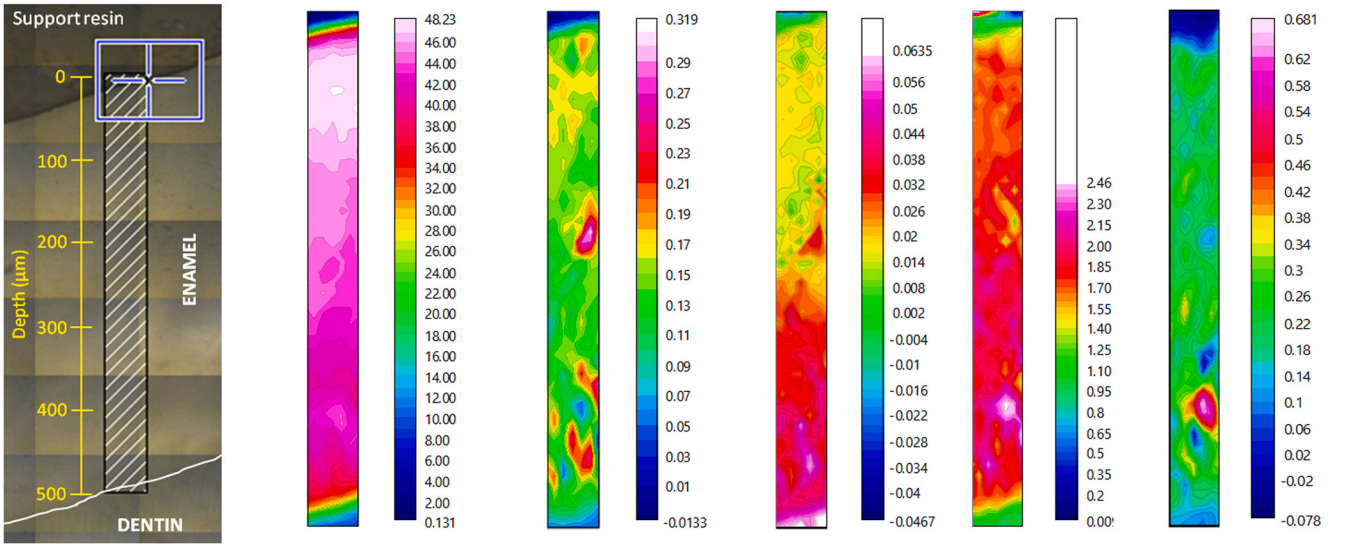

Fig. 2 – Chemical distribution (calculated by peak integration) of carbonates and phosphates in the middle crown of a bovine incisor control tooth (vertical section). The mappings where obtained using OPUS by performing chemical imaging, using peak integration mode A.

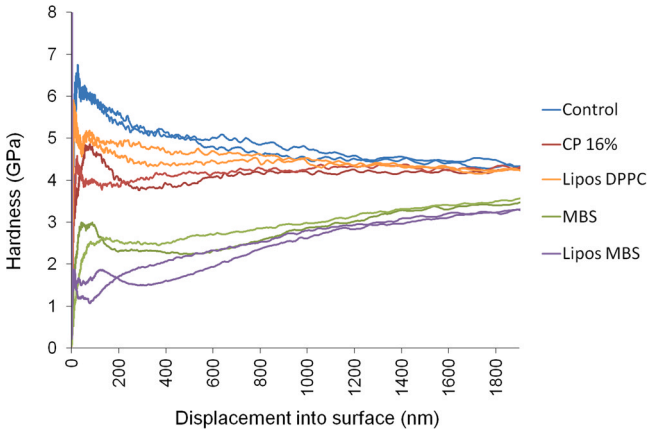

Fig. 3 – Continuous stiffness measurement for the different treatments tested (2 samples per treatment): deionized water (control), Carbamide peroxide at 16% (CP 16%), empty liposomes of DPPC (Lipos DPPC), metabisulfite (MBS) and metabisulfite encapsulated in DPPC liposomes (Lipos MBS).

depth) revealing its presence in the enamel. In the region 1530–1550 cm^{-1}, the highest intensity was found in the dentin region at the bottom of the map, which corresponds to type A carbonates, but also to amide II vibrations, which are found in higher proportion in the dentin.

3.3. *Treatment effects*

3.3.1. *Continuous Stiffness Measurements (CSM)*

It is known that the acid contact with teeth causes partial loss of mineral that results in a reduction of enamel surface hardness [39]. In our work, CSM was used to probe the demineralization caused by MBS as well as the depth reached by this effect, measuring the hardness variations of the enamel from the tooth surface to deeper parts.

CSM analysis (Fig. 3) showed a hardness of about 5 GPa along the depth analyzed (2 µm) for the control. Similar behaviour was observed for CP and DPPC liposomes with a hardness value at around 4.5 GPa. MBS treatment decreased the hardness dramatically especially in the first nanometers, although, a recovery of hardness is observed as the nanoindenter is deepened in the enamel. MBS liposomes also decreased the hardness initially to almost 2 GPa, but also the hardness was increased as depth was gained. Although the analysis has a depth limit set at 2 µm, the observed trend for the last two treatments is that the hardness is progressively recovered. The values observed in the first nanometers of the measurements correspond to the size effect, caused by geometrical dislocation of the HAP crystals when the tip is pressed into the sample [40].

3.3.2. *Treatment effects analyzed by PCA*

According to the results obtained in Section 3.3.1, the first microns were the most affected in terms of mechanical properties since they are the most exposed to the whitening treatments. Nevertheless, the chemicals diffuse into the inner structures, giving chemical structural changes in deeper distances. For this reason, and in order to follow the treatment penetration, single spot µFTIR spectra at 0, 10, 20, 30, 40 and 50 µm depth from the enamel mantel were obtained.

PCA was performed to compare the effect of these changes all over the surface analyzed. The five different treatments were clearly identified from principal component (PC) 1, 2 and 3 (accounting for a total of 99% of the variance) (Fig. 4a). To better relate the observed PCs with the spectra, Fig. 4b represents the average of the 12 spectra corresponding the first 10 µm of enamel of each treatment, since are the most affected. Additionally, Fig. 4c presents the spectra normalized to maximum height to facilitate the appropriate comparison of relative peak intensities and their shifts (Fig. 4c).

As can be observed in the loadings' representation in Fig. 4a, PC1 represents 95.14% of the variation, comprising the whole spectra, especially the phosphate peak. In the scores plot, it can be seen that PC1 (which is negative and thus correspond to the blue parts of the image) did not change for the whole depth analysed in the control sample; for MBS and CP there was a lack of this component in the surface, meaning that the intensity was lower for the first 10 µm deep when compared to control. For DPPC liposomes, it was observed that this treatment also affected the first 10 µm of the enamel, and some of the inner parts were affected by a thin line (as if some liposomes have penetrated the enamel); a higher reflectance intensity in some points of the sample explains the intense blue observed in some parts in the scores map. For MBS liposomes, PC1 showed a high influence in the mantel enamel (most outer part) and then in a thin line entering the inner parts; besides, it can be observed how the whole space is yellow, meaning that the treatment reached the whole surface analysed. In Fig. 4b, the groups MBS, CP, and MBS liposomes showed a reduced reflectance when compared to control, and thus PC1 is related to the reflectance peak intensity. In addition, MBS showed a decrease of the 1058 cm^{-1} intensity, and the contribution of the 1091 cm^{-1} shoulder had almost disappeared. This points out to a clear distortion of the calcium phosphate structure.

PC2 (2.40% of the variance) loading profile presented a peak at 1114 cm^{-1}, placed in the negative part of the loadings.

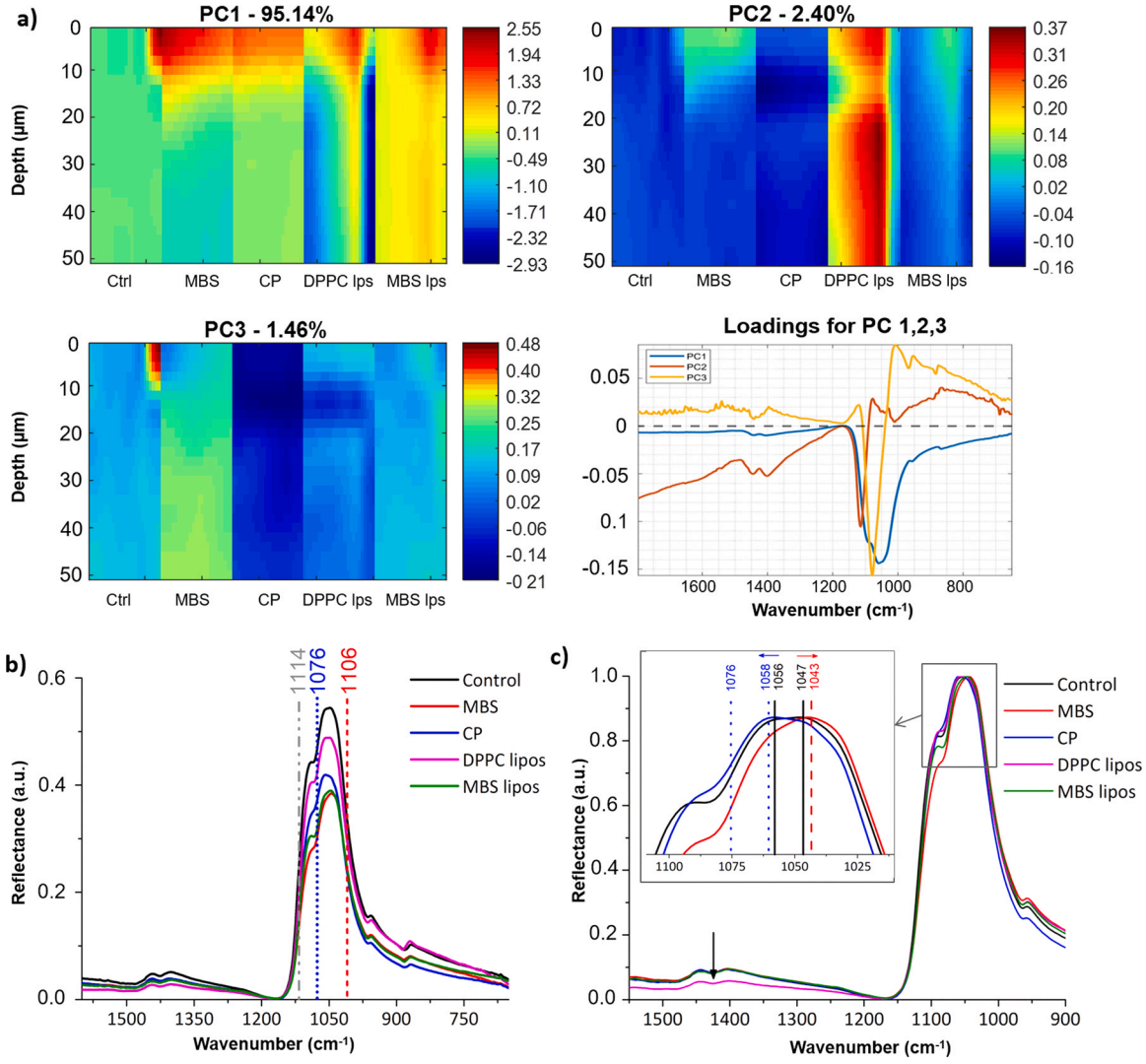

Fig. 4 – (a) Scores (distributed across the enamel depth, starting in the enamel surface at 0–50 µm deep), and loadings for the PCA treatments. (b) Average of the spectra corresponding to the first 10 µm for each treatment (n = 12). (c) Plot b normalized to maximum. Red dash line: MBS shift. Blue dots line, CP shift. Dash and dots grey line: characteristic shoulder of the HAP peak.

It corresponds to the Ca-O-P secondary vibration of ν_1 PO_4^{3-} (reflects changes in the bandwidth) and to the whole ν_2 CO_3^{2-} band. Its presence is related to the blue parts in the corresponding scores map. It can be noticed how the lack of this component was highly significant in DPPC liposomes, and also, although with less intensity, in the first microns of the samples treated with MBS and MBS with liposomes. It is mainly related with a change in the relative intensity of the carbonates since, as indicated in Fig. 4c with a black arrow, for DPPC liposomes it was lower than in the other treatments. Also, all the surface of the CP treated tooth appears blue, meaning that this compound did not affect the carbonates. The phosphate peak corresponding to CP is slightly tightened when compared to the other treatments, that could explain the intense blue in some points of the PC2 scores map since it is also related with the bandwidth.

PC3 (1.46%) loading was negative at 1076 cm^{-1}, i.e. blue in the PC3 scores map, and positive at 1006 cm^{-1} (red in the score map). The first is related to a hypsochromic shift of CP (from 1058 to 1056 cm^{-1}), and the second related to a bathochromic shift of MBS, as can be observed in the specific part of the HAP peak in Fig. 4c. This shift was no observed with the other whitening treatments and represents different chemical interactions with the HAP structure.

4. Discussion

The enamel mapping of the non-treated bovine incisor showed an heterogeneous distribution of the different inorganic species. Physiologically, enamel is an anisotropic material, showing spatial variations in its chemical composition and density [35]. HAP crystals are organized in a basic structural unit called 'rod'. Rods run continuously through all the width of enamel, and close to the dentin become thinner [41]; this creates a mineral gradient, in which the HAP is more packed in the outer enamel, leaving less space for organic matter. The frequencies and the intensity ratio between the

HAP spectrum bands depend on the local environment, and they also vary depending on the modifications on the crystallinity degree [42]. Accordingly, phosphates showed higher reflectance in the outer enamel, where their concentration is higher and the crystal framework is neater, while the reflectance decreased close to the dentin, where the crystals become thinner. Instead, in the inner parts of the enamel carbonates showed higher and the intensity of the HAP peak was reduced. In fact, carbonates modify the lattice parameters of the structure as a consequence of the different size of the substituting ions; the carbonate content increases across outer to inner enamel, which is associated with decreased crystallinity (thus decreased reflectance) and increased solubility [43].

CSM results showed that both, MBS and MBS with liposomes, treatments decreased the enamel hardness beyond 2 µm depth, although the trend revealed that the hardening was partially recovered at larger depth. We related it to erosive demineralization, a process that takes place when the tooth is in contact with a solution that has lower concentration of calcium and phosphate than physiological fluid (plaque fluid), and lower pH than HAP critical pH (5.5). Such damage is characterized by an initial softening of the enamel surface, which extent is reported to be between 0.2 and 3 µm, depending on the immersion time and the acids under study [39]. If the acid contact is maintained, this process is followed by continuous layer-by-layer dissolution of the enamel crystals, leading to a permanent loss of tooth volume. But, if the contact ceases, several salivary protective mechanisms come into play, such as dilution and clearance of the erosive agent from the mouth, neutralization and buffering of acids (within 2–5 min after the exposure), and formation of the acquired pellicle. When the acid is removed, remineralization takes place in the partly demineralized surface enamel.

Considering the sample thickness (around 0.5 cm thick), and the area of the analyzed spots (5 ×5 µm), the presence of the treatment components should not be significant over the signal emitted by the enamel itself when measuring in reflection mode. Therefore, no contribution of liposomes, CP or MBS vibration peaks were expected to be observed, but only the induced modifications in the HAP structure.

The treatments applied produced different effects on the FTIR HAP reflectance spectra. The most important change observed was the decrease in the v_3 PO_4^{3-}, which can be related to a loss of mineral content in the tooth surface [44] (erosion). Kim et al. [24] also observed a decrease in the absorbance, but also an hypsochromic shift of v_3 PO_4^{3-} peak in the acid-eroded enamel. They related these observations to changes in the local structure; in apatite, each P atom is linked to four Ca atoms via a shared oxygen atom (P–O–Ca atomic bridges), and the exposure to acid breaks the Ca–O bonds and consequently reduces the P–O bond length, due to the redistribution of the electron density in the vicinity of the bridging oxygen. According to that, under the acidic conditions of MBS treatments, a decrease in the reflectance due to the acidic nature of MBS (PC1) was observed, but a bathochromic shift, i.e., an elongation took place instead of a shortening of the P-O bond. This could be explained by a SO_4^{2-} substitution of the PO_4^{3-} group; the lattice parameter along the c-axis increases with sulphur substitution because of the length of the atomic bond, as well as an hypsochromic shift happens in the phosphate peak [45]. While, in PC1, MBS affected only the outer layers of the tooth, MBS liposomes affected the whole analysed surface, especially in the middle part; we relate this effect to the increased diffusion promoted by the liposomes [13]. Instead, the bathochromic shift affected only the tooth treated with MBS.

Vasluianu et al. [42], studying the changes induced in HAP by HP whitening treatments, observed a decrease in the reflectance and an hypsochromic shift for the main FITR peaks of HAP; they related it, again, to the shortening of P-O, even if the pH of the treatments was 7.4. In our experiment, CP pH was 8 as in the commercial treatments, since its effectiveness is increased at this pH [46]. Accordingly, a decrease in the reflectance (PC1) and an hypsochromic shift (PC3) were observed. At basic pH, HAP dissolution should not occur, but protein degradation in the tooth organic matrix might be happening. Indeed, the urea in CP along with the ammonium ions (NH_4^+) formed in contact with water act on the hydrogen bonds of the proteins weakening their structure [7]. Since the components of the organic matter form a support structure that stabilizes the crystalline enamel layer [47], any change in the organic matter could cause an effect in the reflectance in the first 30 µm, as observed in PC1. According to Pleshcko et al. [37], a narrowing of the phosphate peak is related with increased crystallinity; this effect was observed for CP treatment, probably because the crystallinity was better detected after the loss of organic matter, because of its better reflective properties.

Regarding the carbonates, MBS treatments promoted the loose of this component at the same extent as it affected the PO_4^{3-} peak (PC1), while CP did not affect the content at all, according to the results observed in the scores map of PC2. This confirms the previous observation, that the mechanism by which the compounds interact with the enamel is different: the first produces an acid attack to the mineral content, the second by promoting the organic matrix decomposition.

5. Conclusions

From the reported results, the following conclusions can be extracted:

MBS treatments soften the first 10 µm of enamel, as happens in the initial states of tooth decay. But, since saliva buffers acid and promotes remineralization once acid contact has been removed, this first microns will be naturally remineralized again.

CP and MBS promote different changes in the HAP mineral; CP shortens the P-O bond while MBS seems to elongate it. Moreover, MBS promotes the loss of carbonates while CP doesn't, which is probably related to the solution's pH.

When comparing MBS and MBS Liposomes, it is observed how liposomes favour the diffusion of MBS to inner layers, since the effects of MBS can be observed in deeper enamel. Thus, the encapsulated MBS whitening effect is highly improved in terms of time when compared to MBS alone or CP.

Acknowledgements

This work was supported by the Spanish Project CTM 2015-65414-C2-1-R; and by the *Universitat Autònoma de Barcelona* with the "*Personal d'Investigació en Formació*" scholarship. The SR-μFTIR experiment was performed at MIRAS beamline at ALBA Synchrotron (Cerdanyola del Vallès, Spain), with the collaboration of ALBA staff (Dr. Ibraheem Yousef). This work has been funded by ALBA Synchrotron through granted proposals (grant references: 2017092361and 2017021987).

REFERENCES

[1] Li Y, Greenwall L. Safety issues of tooth whitening using peroxide-based materials. Br Dent J 2013;215:29–34. https://doi.org/10.1038/sj.bdj.2013.629
[2] Joiner A, Luo W. Tooth colour and whiteness: a review. J Dent 2017;67:S3–10. https://doi.org/10.1016/j.jdent.2017.09.006
[3] Torres C, Crastechini E, Feitosa F, Pucci C, Borges A. Influence of pH on the effectiveness of hydrogen peroxide whitening. Oper Dent 2014;39:E261–8. https://doi.org/10.2341/13-214-L
[4] Kwon SR, Wertz PW. Review of the mechanism of tooth whitening. J Esthet Restor Dent 2015;27:240–57. https://doi.org/10.1111/jerd.12152
[5] Llena C, Martínez-Galdón O, Forner L, Gimeno-Mallench L, Rodríguez-Lozano FJ, Gambini J. Hydrogen peroxide diffusion through enamel and dentin. Materials 2018;11:1–10. https://doi.org/10.3390/ma11091694
[6] Cooper JS, Bokmeyer TJ, Bowles WH. Penetration of the pulp chamber by carbamide peroxide bleaching agents. J Endod 1992;18:315–7.
[7] Goldberg M, Grootveld M, Lynch E. Undesirable and adverse effects of tooth-whitening products: a review. Clin Oral Investig 2010;14:1–10. https://doi.org/10.1007/s00784-009-0302-4
[8] Borges AB, Zanatta RF, Barros ACSM, Silva LC, Pucci CR, Torres CRG. Effect of hydrogen peroxide concentration on enamel color and microhardness. Oper Dent 2015;40:96–101. https://doi.org/10.2341/13-371-L
[9] Soares DG, Basso FG, Pontes ECV, Garcia LDFR, Hebling J, De Souza Costa CA. Effective tooth-bleaching protocols capable of reducing H_2O_2 diffusion through enamel and dentine. J Dent 2014;42:351–8. https://doi.org/10.1016/j.jdent.2013.09.001
[10] Wang Y, Wen X, Jia Y, Huang M, Wang F, Zhang X, et al. Piezo-catalysis for nondestructive tooth whitening. Nat Commun 2020;11:1328. https://doi.org/10.1038/s41467-020-15015-3
[11] Ribeiro JS, Barboza A, da S, Cuevas-Suárez CE, da Silva AF, Piva E, et al. Novel in-office peroxide-free tooth-whitening gels: bleaching effectiveness, enamel surface alterations, and cell viability. Sci Rep 2020;10:1–8. https://doi.org/10.1038/s41598-020-66733-z
[12] Marquillas CB, Procaccini R, Malmagro MV, Sánchez Martín MJ. Breaking the rules: tooth whitening by means of a reducing agent. Clin Oral Invest 2019:1–7. https://doi.org/10.1007/s00784-019-03140-3
[13] Babot-Marquillas C, Sánchez-Martín MJ, Rodríguez-Martínez J, Estelrich J, Busquets MA, Valiente M. Flash tooth whitening: a friendly formulation based on a nanoencapsulated reductant. Colloids Surf B Biointerfaces 2020;195:111241https://doi.org/10.1016/j.colsurfb.2020.111241
[14] Wang C, Li Y, Wang X, Zhang L, Tiantang FuB. The enamel microstructures of bovine mandibular incisors. Anat Rec 2012;295:1698–706. https://doi.org/10.1002/ar.22543
[15] Standardization IO for. ISO 28399:2020 Dentistry — External tooth bleaching products. 2020.
[16] Dumas P, Sockalingum GD, Sulé-Suso J. Adding synchrotron radiation to infrared microspectroscopy: what's new in biomedical applications? Trends Biotechnol 2007;25:40–4. https://doi.org/10.1016/j.tibtech.2006.11.002
[17] Miller LM, Dumas P. Chemical imaging of biological tissue with synchrotron infrared light. Biochim Biophys Acta Biomembr 2006;1758:846–57. https://doi.org/10.1016/j.bbamem.2006.04.010
[18] Fan K, Bell P, Fried D. Rapid and conservative ablation and modification of enamel, dentin, and alveolar bone using a high repetition rate transverse excited atmospheric pressure CO[sub 2] laser operating at λ=9.3 μm. J Biomed Opt 2006;11:064008https://doi.org/10.1117/1.2401151
[19] Efeoglu N, Wood D, Efeoglu C. Microcomputerised tomography evaluation of 10% carbamide peroxide applied to enamel. J Dent 2005;33:561–7. https://doi.org/10.1016/j.jdent.2004.12.001
[20] Ryman BE, Tyrrell DA. Liposomes - methodology and applications. Front Biol 1979;48:549–74.
[21] Nicolas J, RibÃ3 L, Colldelram C, Crisol A, Dumas P, Ellis G, et al. Mechanical design of MIRAS, infrared microspectroscopy beam line at ALBA synchrotron. JACoW Geneva, Switz 2017:403–8. https://doi.org/10.18429/jacow-medsi2016-fraa03
[22] Amigo JM, Babamoradi H, Elcoroaristizabal S. Hyperspectral image analysis. A tutorial. Anal Chim Acta 2015;896:34–51. https://doi.org/10.1016/j.aca.2015.09.030
[23] Mobaraki N, Amigo JM. HYPER-Tools. A graphical user-friendly interface for hyperspectral image analysis. Chemom Intell Lab Syst 2018;172:174–87. https://doi.org/10.1016/j.chemolab.2017.11.003
[24] Kim IH, Son JS, Min BK, Kim YK, Kim KH, Kwon TY. A simple, sensitive and non-destructive technique for characterizing bovine dental enamel erosion: attenuated total reflection Fourier transform infrared spectroscopy. Int J Oral Sci 2016;8:54–60. https://doi.org/10.1038/ijos.2015.58
[25] Bachmann L, Diebolder R, Hibst R, Zezell DM. Infrared absorption bands of enamel and dentin tissues from human and bovine teeth. Appl Spectrosc Rev 2003;38:1–14. https://doi.org/10.1081/ASR-120017479
[26] Arboleda A, Franco M, Caicedo J, Tirado L, Goyes C. Synthesis and chemical and structural characterization of hydroxyapatite obtained from eggshell and tricalcium phosphate. Ing y Compet 2016;18:69. https://doi.org/10.25100/iyc.v18i1.2178
[27] Gadaleta SJ, Paschalis EP, Betts F, Mendelsohn R, Boskey AL. Fourier transform infrared spectroscopy of the solution-mediated conversion of amorphous calcium phosphate to hydroxyapatite: new correlations between X-ray diffraction and infrared data. Calcif Tissue Int 1996;58:9–16. https://doi.org/10.1007/BF02509540
[28] Lopes CCA, Limirio PHJO, Novais VR, Dechichi P. Fourier transform infrared spectroscopy (FTIR) application chemical characterization of enamel, dentin and bone. Appl Spectrosc Rev 2018;53:747–69. https://doi.org/10.1080/05704928.2018.1431923
[29] Gross K, Yang TC, Kareiva A. Curr Biol CB 2014;24:503–6. https://doi.org/10.1039/c4ce00119b
[30] Rokaya D, Srimaneepong V, Sapkota J, Qin J, Siraleartmukul K, Siriwongrungson V. Polymeric materials and films in dentistry: an overview. J Adv Res 2018;14:25–34. https://doi.org/10.1016/j.jare.2018.05.001

[31] Chen KH, Cheng WT, Li MJ, Yang DM, Lin SY. Calcification of senile cataractous lens determined by Fourier transform infrared (FTIR) and Raman microspectroscopies. J Microsc 2005;219:36–41. https://doi.org/10.1111/j.1365-2818.2005.01491.x
[32] Fleet M. Biological Apatites. Carbonated Hydroxyapatite Mater. Synth. Appl. Pan Standford Publishing; 2015. p. 199–234.
[33] Brangule A, Gross KA. Importance of FTIR spectra deconvolution for the analysis of amorphous calcium phosphates. IOP Conf Ser Mater Sci Eng 2015:77. https://doi.org/10.1088/1757-899X/77/1/012027
[34] Beniash E, Stifler CA, Sun CY, Jung GS, Qin Z, Buehler MJ, et al. The hidden structure of human enamel. Nat Commun 2019;10:1–13. https://doi.org/10.1038/s41467-019-12185-7
[35] Sakae T. Variations in dental enamel crystallites and microstructure. J Oral Biosci 2006;48:85–93. https://doi.org/10.2330/joralbiosci.48.85
[36] Verdelis K, Crenshaw MA, Paschalis EP, Doty S, Atti E, Boskey AL. Spectroscopic imaging of mineral maturation in bovine dentin. J Dent Res 2003;82:697–702. https://doi.org/10.1177/154405910308200908
[37] Pleshko N, Boskey A, Mendelsohn R. Novel infrared spectroscopic method for the determination of crystallinity of hydroxyapatite minerals. Biophys J 1991;60:786–93. https://doi.org/10.1016/S0006-3495(91)82113-0
[38] Sydney-Zax M, Mayer I, Deutsch D. Carbonate content in developing human and bovine enamel. J Dent Res 1991;70:913–6. https://doi.org/10.1177/00220345910700051001
[39] Lussi A, Schlueter N, Rakhmatullina E, Ganss C. Dental erosion - an overview with emphasis on chemical and histopathological aspects. Caries Res 2011;45:2–12. https://doi.org/10.1159/000325915
[40] Voyiadjis GZ, Yaghoobi M. Review of nanoindentation size effect: experiments and atomistic simulation. Crystals 2017;7:8–10. https://doi.org/10.3390/cryst7100321
[41] Shahmoradi M, Bertassoni LE, M. Elfallah H, Swain M. Fundamental structure and properties of enamel, dentin and cementum Mahdi. DAdv Calcium Phosphate Biomater 2014;vol. 2:1–39. https://doi.org/10.1007/978-3-642-53980-0
[42] Vasluianu R, Forna DA, Zaltariov M, Murariu A. *In vitro* study using ATR-FTIR method for analyze the effects of the carbamide peroxide on the dental structure. Rev Chim 2016;67:2475–8.
[43] Xu C, Reed R, Gorski JP, Wang Y, Walker MP. The distribution of carbonate in enamel and its correlation with structure and mechanical properties. J Mater Sci 2012;47:8035–43. https://doi.org/10.1007/s10853-012-6693-7
[44] González-López S, Torres-Rodríguez C, Bolaños-Carmona V, Sanchez-Sanchez P, Rodríguez-Navarro A, Álvarez-Lloret P, et al. Effect of 30% hydrogen peroxide on mineral chemical composition and surface morphology of bovine enamel. Odontology 2016;104:44–52. https://doi.org/10.1007/s10266-014-0189-7
[45] Tran LK, Stepien KR, Bollmeyer MM, Yoder CH. Substitution of sulfate in apatite. Am Miner 2017;102:1971–6. https://doi.org/10.2138/am-2017-6088
[46] Young N, Fairley P, Mohan V, Jumeaux C. A study of hydrogen peroxide chemistry and photochemistry in tea stain solution with relevance to clinical tooth whitening. J Dent 2012;40:e11–6. https://doi.org/10.1016/j.jdent.2012.07.016
[47] Mcguire JD, Walker MP, Dusevich V, Wang Y, Gorski JP. Dentin enamel junction. Connect Tissue Res 2014;55:33–7. https://doi.org/10.3109/03008207.2014.923883